

Sofia Gourtsoyianni  
Nickolas Papanikolaou  
Spyros Yarmenitis  
Thomas Maris  
Apostolos Karantanias  
Nicholas Gourtsoyiannis

## Respiratory gated diffusion-weighted imaging of the liver: value of apparent diffusion coefficient measurements in the differentiation between most commonly encountered benign and malignant focal liver lesions

Received: 23 March 2007  
Revised: 3 July 2007  
Accepted: 26 September 2007  
Published online: 10 November 2007  
© European Society of Radiology 2007

**Abstract** The purpose of this study was to measure apparent diffusion coefficient values of normal liver parenchyma and focal liver lesions utilizing a respiratory gated diffusion sequence with multiple b-values and to investigate whether apparent diffusion coefficient (ADC) measurements may be utilized to characterize and differentiate between malignant and benign focal hepatic lesions. Thirty-eight consecutive patients underwent MRI of the liver including diffusion-weighted imaging (DWI). A single-shot echo planar imaging sequence was applied in coronal orientation with multiple b-values (0, 50, 500, 1,000 s/mm<sup>2</sup>) and respiratory gating. ADC values were recorded on corresponding maps utilizing region of interest measurements in patients with benign (group A), malignant (group B) focal lesions and liver parenchyma (group C). Statistical analysis was applied to check whether differences in mean ADC values were significant ( $p < 0.05$ ). No focal lesions were detected in 11 patients, with a mean ADC value (CI 95%) of liver parenchyma  $1.25 \times 10^{-3}$  mm<sup>2</sup>/s ( $1.21 \times$

$10^{-3}$  mm<sup>2</sup>/s– $1.29 \times 10^{-3}$  mm<sup>2</sup>/s). Differences in mean ADC of liver parenchyma between group A and B were not significant ( $p = 0.054$ ,  $1.30 \times 10^{-3}$  mm<sup>2</sup>/s and  $1.31 \times 10^{-3}$  mm<sup>2</sup>/s, respectively). Mean ADC value (95% CI) of 22 benign lesions found in 18 patients was  $2.55 \times 10^{-3}$  mm<sup>2</sup>/s ( $2.35 \times 10^{-3}$  mm<sup>2</sup>/s– $2.74 \times 10^{-3}$  mm<sup>2</sup>/s), while the mean ADC value (95% CI) of 16 malignant lesions recorded in 9 patients was  $1.04 \times 10^{-3}$  mm<sup>2</sup>/s ( $0.9 \times 10^{-3}$  mm<sup>2</sup>/s– $1.17 \times 10^{-3}$  mm<sup>2</sup>/s). The difference between mean ADC values of benign and malignant focal lesions was statistically significant ( $p < 0.0001$ ). Respiratory gated diffusion-weighted imaging in the liver is technically feasible. Apparent diffusion coefficient measurements can be useful in differentiating malignant from benign focal liver lesions.

**Keywords** Diffusion-weighted imaging · Liver · Magnetic resonance · Tissue characterization · Respiratory gating

S. Gourtsoyianni · N. Papanikolaou ·  
S. Yarmenitis · A. Karantanias ·  
N. Gourtsoyiannis (✉)  
Department of Radiology,  
University Hospital of Heraklion,  
71110 Stavrakia,  
Heraklion/Crete, Greece  
e-mail: gournick@med.uoc.gr  
Tel.: +30-2810-392541  
Fax: +30-2810-542095

T. Maris  
Department of Medical Physics,  
University Hospital of Heraklion,  
Medical School of Crete,  
Heraklion/Crete, Greece

### Introduction

Diffusion-weighted imaging (DWI) is widely appreciated as an indispensable tool in the examination of the central nervous system and is used nowadays routinely not only for the detection of acute ischemic stroke, but also for the characterization and differentiation of brain tumors and intracranial infections [1–3]. Only recently, several efforts

were undertaken to apply DWI in the abdomen, especially for the detection of malignant lesions in organs such as the prostate, the bladder and the rectum [4–8].

One of the most important technical challenges in abdominal DWI is to minimize geometrical distortions and susceptibility artifacts that are generated due to the presence of bones and air. Recently, with the advent of parallel imaging algorithms, such a task can be accom-

**Table 1** The most important parameters of single shot diffusion echo planar imaging sequence applied with respiratory gating are shown

Sequence parameters	
Acquisition duration* (ms)	1,300
Echo time (ms)	67
GRAPPA factor	3
Slice thickness (mm)	8
Field of view (mm×mm)	400×400
Matrix	128×128 (interpolated to 256×256)
Phase encoding direction	Foot-head

\*Acquisition duration is the actual scanning time during apnea between two successive respiratory cycles

plished to a certain extent [9]. Breath-hold echo planar sequences were applied for diffusion studies of the abdomen [9–11]; however, certain limitations in terms of spatial resolution and signal-to-noise ratio (SNR) were present due to acquisition time constraints. Respiratory gated sequences have the advantage of increased SNR due to multiple averages that can be acquired. This increased SNR may be exploited in favor of increased spatial resolution. The differential diagnosis between malignant and benign focal liver lesions remains a diagnostic challenge, for which different modalities and methodologies within modalities have been proposed, including multi-phasic contrast-enhanced CT [12] and MRI [13], CT portography [14] and perfusion studies using dedicated US contrast agents [15]. Diffusion is a novel contrast mechanism that is directly related to the size of extracellular space. Therefore, it is possible to identify lesion hypercellularity based on the diffusion pattern that it exhibits on DW images [16, 17]. Benign lesions such as hemangiomas

are characterized by an enlargement of the extracellular space compared to normal tissue, while cysts contain mostly free moving protons. As a result such lesions are expressed with free diffusion and elevated apparent diffusion coefficient (ADC) values. In the majority of malignant lesions, hypercellularity results in shrinkage of the extracellular space, leading to restricted diffusion and thus decreased ADC values, with the exception of necrotic areas where the loss of tissue architecture may lead to elevation of ADC values.

The aim of this study was to: (1) introduce a respiratory gated diffusion sequence and obtain quantitative measurements of the apparent diffusion coefficient of normal liver parenchyma and focal liver lesions and (2) investigate whether ADC values obtained with the respiratory gated diffusion sequence can be used to characterize and differentiate between malignant and most commonly encountered benign focal liver lesions.

## Materials and methods

The study comprised 38 consecutive patients, 10 males and 28 females, with an age range of 22–78 years and a mean age of 58.12 years, who were referred for an abdominal MRI examination of the liver. The clinical question was to rule out presence of pathology in the liver, adrenal glands, spleen, pancreas or kidneys. The final diagnosis was established by MR imaging findings (T2-weighted and dynamic post-gadolinium T1-weighted images) and clinical follow-up. Patients were classified into three groups according to final diagnosis. Group A was comprised of patients with the most commonly encountered benign focal liver lesions, such as liver cysts and hepatic hemangiomas. Group B consisted of

**Fig. 1** Coronal DWI with multiple b values and ADC map on a patient with a large liver cyst. **a** The lesion exhibits high signal intensity on b=0 (**a**) and b=50 (**b**), while the signal is significantly decreased on the b=1,000 (**c**). ADC map (**d**) confirms that the lesion exhibits an elevated ADC value relative to normal liver parenchyma mainly due to the presence of free moving water

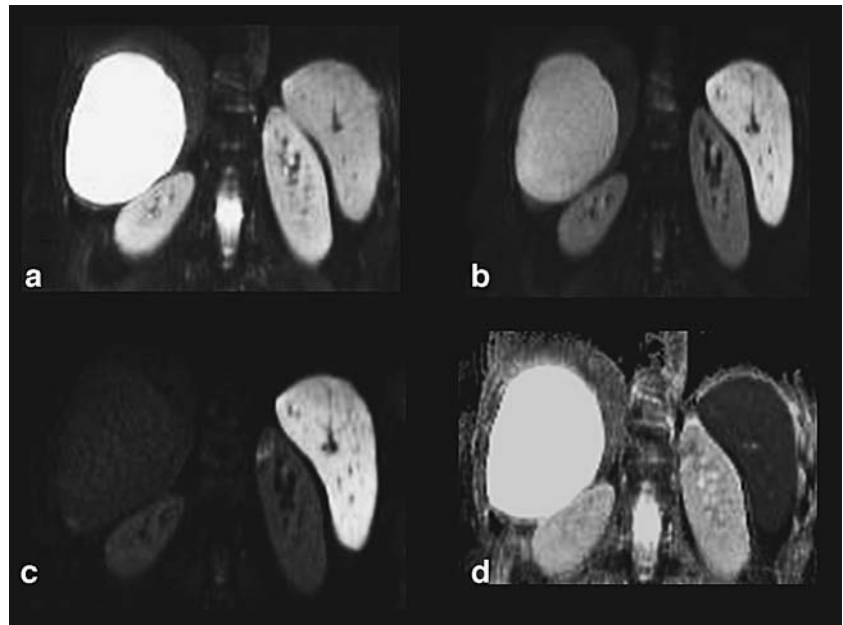


**Table 2** Mean ADC values and 95% CI shown in parenthesis of focal liver lesions

Lesions (number)	Mean ADC ( $\times 10^{-3}$ mm <sup>2</sup> /s) 95% CI
Cysts (n=15)	2.55 (2.27–2.84)
Hemangiomas (n=7)	1.90 (1.56–2.24)
HCC (n=2)	1.38 (0.23–2.52)
Metastases (n=13)	0.99 (0.86–1.11)

patients with malignant focal liver lesions, including liver metastases and hepatocellular carcinoma. In cases with multiple metastatic lesions, only four of them were selected for quantitative measurements. Selection criteria when multiple lesions were present were based on size, morphology and location. The four largest in size, with the smallest measuring 1.4 cm in diameter, most conspicuous lesions located in the right liver lobe were selected. Group C consisted of patients without any liver abnormalities.

### MRI examination protocol

All patients were examined on a 1.5-T MR scanner (SonataVision, Siemens Medical Solutions, Erlangen, Germany) with a high performance gradient system capable of reaching a maximum amplitude of 40 mT/m and a slew rate of 200 mT/m/ms, using two four-element phased array body coils and a six-element spine array coil. In addition to our standard upper abdomen protocol comprising axial three-dimensional spoiled gradient echo (VIBE) sequence (pre and post contrast at 30 s, 60 s, 120 s and 5 min), axial T2-weighted turbo spin echo with fat saturation and respiratory triggering technique, a coronal SS EPI sequence was applied with four different b values

(0, 50, 500 and 1,000 s/mm<sup>2</sup>). Significantly fewer geometrical distortions were present on coronal orientation; therefore, this plane was selected. Respiratory gating was utilized in order to overcome motion artifacts. Echo time of 67 ms was achieved by means of parallel imaging GRAPPA algorithm and an acceleration factor of 3. Cardiac or pulse synchronization was not mandatory, due to utilization of a single shot EPI sequence. The most important sequence parameters are shown in Table 1. Signal-to-noise ratio (SNR) of the normal liver was measured utilizing the equation:

$$\text{SNR}_{\text{liver}} = \frac{SI_{b1000}}{\text{noise}_{b1000}}$$

where  $SI_{b1000}$  corresponds to the mean signal intensity recorded by means of four ROIs placed at the periphery of the right liver lobe on b1000 image, and  $\text{noise}_{b1000}$  is equal to the standard deviation of a measurement performed in the air (upper left corner) on the b1000 image.

Apparent diffusion coefficient (ADC) maps were generated on the main MR console using dedicated post-processing software (Siemens Medical Solutions, Erlangen, Germany). ADC values were calculated according to the following formula:

$$SI_b = SI_{b0} * \exp(-b * \text{ADC})$$

where  $SI_b$  corresponds to the signal intensity measured on a specific b-value image, while  $SI_{b0}$  is the signal intensity on the b0 image. ADC measurements were performed by placing ROIs on ADC maps on different focal liver lesions as well as on areas of parenchyma. In case of different

**Fig. 2** Coronal SE EPI diffusion images in a patient with pancreatic carcinoma and liver metastasis. Three b-values are shown, b=0 (a), b=50 (b) and b=1,000 (c). The metastatic lesions (arrow) exhibit high signal intensity on the heavily diffusion-weighted image (c) and low signal intensity on the ADC map (d). These imaging features can be explained in the basis of restricted diffusion due to hypercellularity of the lesion

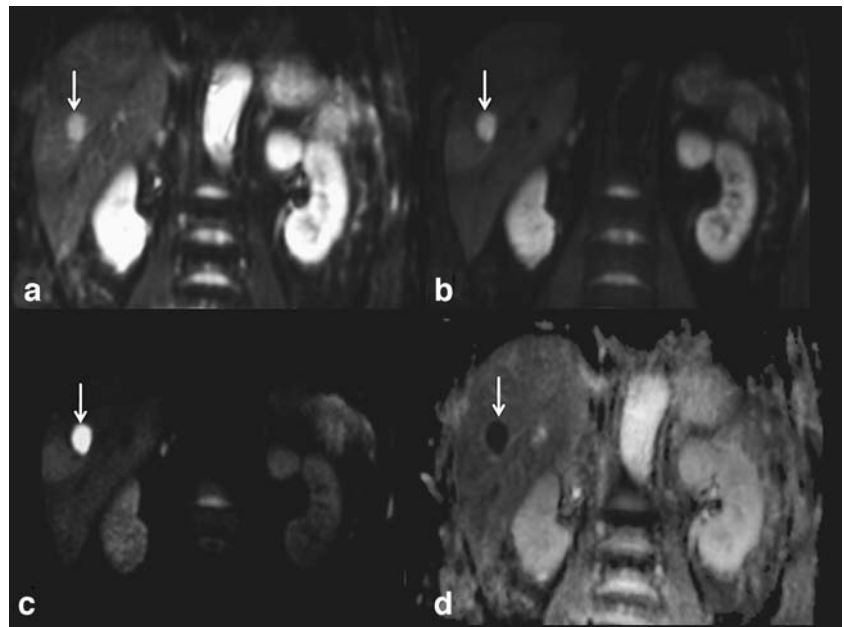
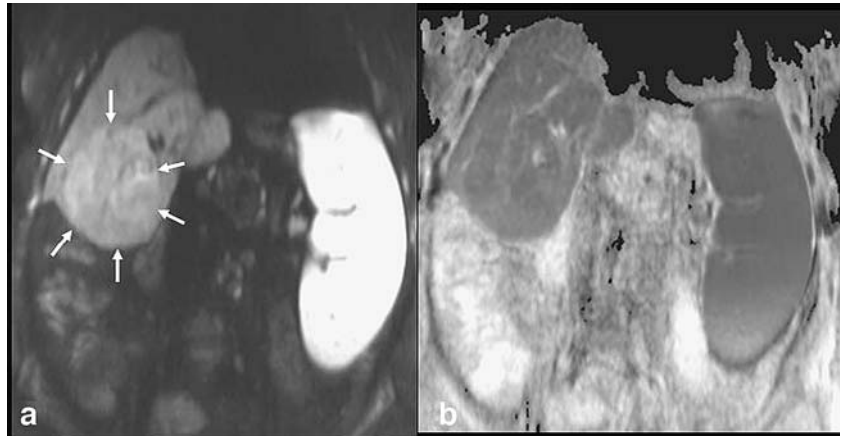


**Fig. 3** Coronal SE\_EPI diffusion image (a) and ADC map (b) in a patient with hepatocellular carcinoma. The lesion (arrows) is presented with similar ADC value to liver parenchyma with some areas with increased cellularity presented with high signal intensity on b1000 and low ADC values



signal behavior in the periphery and center of lesions on ADC maps, measurements were performed in both sites. In cases with parenchyma ROIs were placed so as to avoid visible vessels. Mean ADC values of focal liver lesions and normal liver parenchyma were recorded, and the Mann-Whitney test was applied to check whether mean ADC values between most commonly encountered benign (group A) and malignant (group B) lesions, as well as between liver parenchyma measured in all three groups were statistically significant. A receiver operating characteristic (ROC) curve analysis was used to define the ADC cutoff value for differentiating benign from malignant focal liver lesions and hemangiomas from metastases.

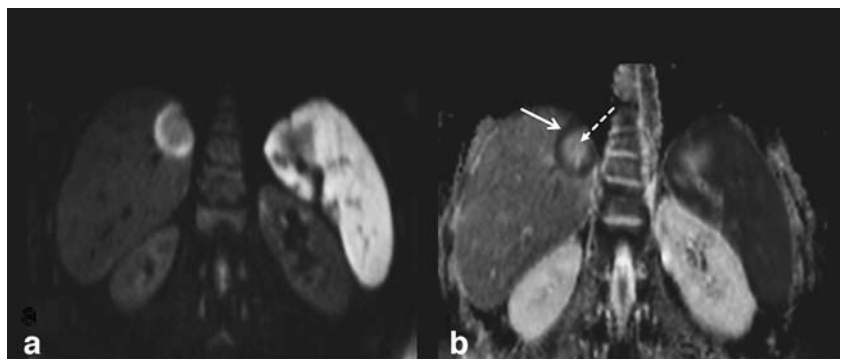
## Results

All focal liver lesions were located at segments V–VIII of the right liver lobe with a mean size of 8.3 mm in maximum diameter. Mean SNR of the liver measured on the respiratory gated diffusion sequence applied in the current study was 32.15 (standard deviation: 4.3). No abnormality was found in liver parenchyma in 11 patients. Seven hemangiomas were depicted in 7 patients, and 15 cysts were shown in 11 patients. One patient presented with four cysts and another with two, while two patients had both a cyst and a hemangioma. Two patients, both with known cirrhosis due to hepatitis C and B, respectively, were found

to have hepatocellular carcinoma, which was proven by follow-up studies. Finally, 13 metastatic lesions were demonstrated in 7 patients, resulting from different primary malignancies including 1 patient with an unknown primary. The sigmoid colon, rectum, pancreas, small bowel, lung and breast were the sites of primary carcinomas in six patients. Benign cysts demonstrated a significant signal loss in the b value of 1,000 s/mm<sup>2</sup> that was compatible with increased ADC on the corresponding map in all cases (Fig. 1). Mean ADC value of cysts was found to be  $2.55 \times 10^{-3}$  mm<sup>2</sup>/s (Table 2). Hemangiomas showed a similar signal behavior with the cysts on DWI, while ADC maps demonstrated an inhomogeneous appearance in some of the cases, most probably corresponding to fibrosis or the presence of thrombus. Mean ADC value of hemangiomas was found to be  $1.9 \times 10^{-3}$  mm<sup>2</sup>/s (Table 2).

Metastatic lesions exhibited increased signal intensity in all four b values, compatible with restricted diffusion as confirmed on ADC maps (Fig. 2). Mean ADC value of metastases was found to be  $0.99 \times 10^{-3}$  mm<sup>2</sup>/s, while that of HCC was  $1.38 \times 10^{-3}$  mm<sup>2</sup>/s (Fig. 3; Table 2). Two different imaging patterns were recognized on ADC maps. Metastatic lesions from colorectal, breast and lung primaries presented with a ring-like pattern featuring a low ADC in the periphery (mean value: 1.048, standard deviation: 0.22), and a high ADC value in the center (mean value: 1.43, standard deviation: 0.13). The latter corresponded to central necrosis (Fig. 4), as confirmed on T2-weighted and

**Fig. 4** Patient with colorectal carcinoma and liver metastasis. A bright peripheral rim with a central area of low signal intensity is demonstrated on the image with b=1,000 (a). ADC map (b) shows the peripheral rim with low ADC value most probably representing active tumor areas (arrow), while the central area exhibits a high ADC value compatible with necrosis (dotted arrow)



post gadolinium T1-weighted images. In ring-like lesions ADC values were measured at the periphery. Metastatic lesions from pancreatic, small bowel malignancies and unknown primary presented with a homogeneously low ADC value.

In 13 patients without focal liver lesions (group C), the mean ADC value of liver parenchyma was  $1.25 \times 10^{-3} \text{ mm}^2/\text{s}$ . The mean ADC values of liver parenchyma in 16 patients presented with benign liver lesions (group A) and 9 patients presented with malignant liver lesions (group B) were  $1.30 \times 10^{-3} \text{ mm}^2/\text{s}$  and  $1.31 \times 10^{-3} \text{ mm}^2/\text{s}$ , respectively (Table 3). Differences in mean ADC values of liver parenchyma between all groups were not significant (group A versus B,  $p=0.054$ , group B versus C,  $p=0.18$ , and group A versus C,  $p=0.065$ ).

Mean ADC value of 22 benign lesions found in 18 patients was  $2.55 \times 10^{-3} \text{ mm}^2/\text{s}$ , while mean ADC value of 16 malignant lesions found in 9 patients was  $1.04 \times 10^{-3} \text{ mm}^2/\text{s}$  (Table 3). The differences between mean ADC values of benign and malignant focal liver lesions were statistically significant ( $p<0.0001$ ) (Fig. 5). According to ROC curve analysis, ADC measurements were capable of differentiating between benign and malignant liver lesions with a diagnostic accuracy of 1.0 (95% CI: 0.904 to 1.000), sensitivity and specificity of 100% using a cutoff ADC value of  $1.47 \times 10^{-3} \text{ mm}^2/\text{s}$ . Metastatic lesions presented with significantly lower ADC values compared to cysts ( $p<0.0001$ ) and hemangiomas ( $p<0.0001$ ) (Fig. 6). Cysts presented with significantly higher ADC values than hemangiomas ( $p<0.001$ ). For the differentiation between hemangiomas and metastatic lesions, ROC curve analysis revealed that ADC measurements had a diagnostic accuracy, as given by the area under the curve, of 1.000 (95% CI: 0.830 to 1.000) with a sensitivity and a specificity of 100% using a cutoff ADC value of  $1.26 \times 10^{-3} \text{ mm}^2/\text{s}$ .

## Discussion

With the ongoing advent of technology, nowadays radiologists are able to provide clinicians with more

**Table 3** Mean ADC values and 95% CI shown in parenthesis of liver parenchyma, benign and malignant liver lesions

	Mean ADC ( $\times 10^{-3} \text{ mm}^2/\text{sec}$ )	95% CI
Liver parenchyma group A (n=16)	1.30	(1.25–1.34)
Liver parenchyma group B (n=9)	1.31	(1.2–1.41)
Liver parenchyma group C (n=13)	1.25	(1.21–1.29)
Benign liver lesions (n=22)	2.55	(2.35–2.74)
Malignant liver lesions (n=13)	1.04	(0.9–1.17)

Group A: patients with benign focal liver lesions  
Group B: patients with malignant focal liver lesions  
Group C: patients with no focal liver lesions

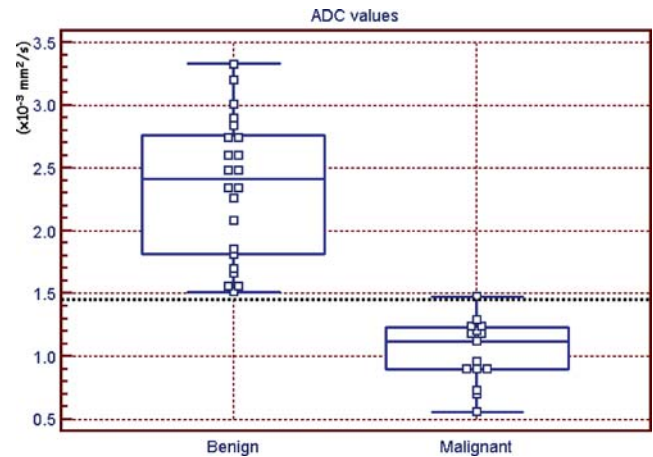


**Fig. 5** Box plot of ADC values calculated for 22 benign and 15 malignant lesions. Dotted line represents the optimal cutoff ADC value of  $1.47 \times 10^{-3} \text{ mm}^2/\text{s}$  to differentiate benign from malignant liver lesions

information regarding liver pathology than ever before. On the other hand the imaging assessment of routine clinical cases is becoming more demanding and complex mainly due to the fact that novel therapeutic treatments are applied and there is a shift towards a new paradigm. Non-invasive imaging will intervene earlier in the patient pathway providing detailed information on tumor grade, prognosis and appropriate treatment as well as in assessing therapeutic response.

Diffusion is a novel contrast mechanism that recently has gained significant attention in oncologic imaging [18]. This new technique has so far been shown to be capable of detecting subtle alterations in the microarchitecture of the tissue and therefore has the potential to improve lesion characterization [19]. Several technical limitations prohibiting routine application of diffusion in the liver have been overcome by recent technical advances. The main purpose of

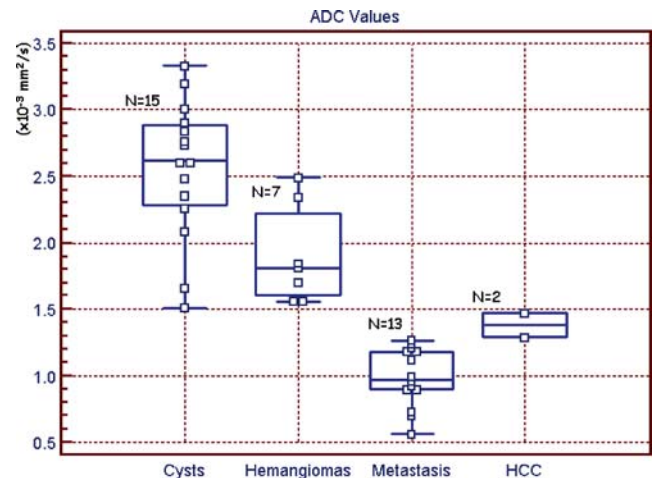


**Fig. 6** Box plot showing the ADC values for each type of focal liver lesions

the current study was to assess the feasibility of the technique and evaluate its potential in differentiating malignant from benign lesions based on ADC measurements.

Previous studies reported the capability of diffusion in differentiating benign from malignant focal liver lesions by measuring the ADCs [20, 21]. All studies showed lower ADC values in malignant than in benign lesions, some of them with significant overlap. However, different b-values were utilized to calculate ADCs, leading to confusion on the optimal number and range of b-values that should be used to quantify the ADC. The DWI sequence utilized in the current study comprised multiple b-values, both low and high, to be able to improve the accuracy of the ADC quantification. It is well known that ADC quantification based on low to moderate b values ( $<500$  s/mm<sup>2</sup>) suffers from perfusion effects, while to overcome this limitation higher b-values should be considered. However, a certain limitation to that extent is the poor signal-to-noise ratio (SNR) that can be achieved on high b-value DWI images. In the current study, the sequence implementation with multiple averages and respiratory gating resulted in adequate SNR even in high b-value images. In addition, the signal pattern of liver lesions presented on ADC maps was taken into consideration when measuring ADC values. In case of a ring-like appearance of lesions on ADC maps, ADC measurements from the periphery of the lesions rather than the center were included in the statistical analysis to reduce any potential overlap with most commonly encountered benign lesions due to the higher ADC values measured in the central areas of such lesions. Although the patient sample examined in the current study was rather inhomogeneous, ADC measurements were significantly different between benign and malignant

focal liver lesions as proved by ROC curve analysis. Our findings are in close agreement with others [17] regarding the mean ADC values calculated for metastatic lesions and HCCs. However, in the current study, hemangiomas presented with lower ADC values. The latter can be explained by the smaller b-values utilized by other studies [17]. The results of this study confirmed the potential of ADC measurements to differentiate benign from malignant liver lesions with a sensitivity and specificity of 100%. The utilization of a respiratory gated sequence offering increased SNR even in high b-value images might explain the higher sensitivity and specificity values that resulted in this study.

A study limitation is the lack of cases with focal nodular hyperplasia (FNH). Their absence in the current study outweighed the differences of ADC values between malignant and benign lesions due to the fact that FNH, being a hypercellular lesion, is expected to present with low ADC values. It remains to be examined on larger series whether it will be possible to predict the type of metastasis based on diffusion imaging characteristics of the lesion, especially in case of metastases due to unknown primary.

## Conclusions

Quantitative measurements of ADC values can be performed successfully on maps based on coronal diffusion-weighted images using a maximum b value of 1,000 when parallel imaging and respiratory gating are used. Quantification of ADC values can be useful in differentiating malignant from most commonly encountered benign focal liver lesions.

## References

- Moseley ME, Kucharczyk J, Mintorovitch J et al (1990) Diffusion weighted MR imaging of acute stroke: correlation with T2-weighted and magnetic susceptibility-enhanced MR imaging in cats. *AJNR Am J Neuroradiol* 11:423–429
- Provenzale JM, Mukundan S, Barboriak DP (2006) Diffusion-weighted and perfusion MR imaging for brain tumor characterization and assessment of treatment response. *Radiology* 239(3):632–649
- Dorenbeck U, Butz B, Schlaier J, Bretschneider T, Schuierer G, Feuerbach S (2003) Diffusion weighted echo-planar MRI of the brain with calculated ADCs: a useful tool in the differential diagnosis of tumor necrosis from abscess? *J Neuroimaging* 13(4):330–338
- Tanimoto A, Nakashima J, Kohno H, Shinmoto H, Kuribayashi S (2007) Prostate cancer screening: the clinical value of diffusion-weighted imaging and dynamic MR imaging in combination with T2-weighted imaging. *J Magn Reson Imaging* 25(1):146–152
- Matsuki M, Inada Y, Tatsugami F, Tanikake M, Narabayashi I, Katsuoka Y (2007) Diffusion-weighted MR imaging for urinary bladder carcinoma: initial results. *Eur Radiol* 17(1):201–204
- Thoeny HC, De Keyzer F (2007) Extracranial applications of diffusion-weighted magnetic resonance imaging. *Eur Radiol* 17(6):1385–1393
- Nasu K, Kuroki Y, Kuroki S, Murakami K, Nawano S, Moriyama N (2004) Diffusion-weighted single shot echo planar imaging of colorectal cancer using a sensitivity-encoding technique. *Jpn J Clin Oncol* 34(10):620–626
- Squillaci E, Manenti G, Cova M, Di Roma M, Miano R, Palmieri G, Simonetti G (2004) Correlation of diffusion-weighted MR imaging with cellularity of renal tumours. *Anticancer Res* 24(6):4175–4179
- Yoshikawa T, Kawamitsu H, Mitchell DG, Ohno Y, Ku Y, Seo Y, Fujii M, Sugimura K (2006) ADC measurement of abdominal organs and lesions using parallel imaging technique. *Am J Roentgenol* 187(6):1521–1530
- Yamada I, Aung W, Himeno Y, Nakagawa T, Shibuya H (1999) Diffusion coefficients in abdominal organs and hepatic lesions: evaluation with intravoxel incoherent motion echo-planar MR imaging. *Radiology* 210:617–623

11. Kim T, Murakami T, Takahashi S, Hori M, Tsuda K, Nakamura H (1999) Diffusion-weighted single-shot echo-planar MR imaging for liver disease. *Am J Roentgenol* 173:393–398
12. Semelka RC, Martin DR, Balci C, Lance T (2001) Focal liver lesions: comparison of dual-phase CT and multisequence multiplanar MR imaging including dynamic gadolinium enhancement. *J Magn Reson Imaging* 13(3):397–401
13. Pirovano G, Vanzulli A, Marti-Bonmati L, Grazioli L, Manfredi R, Greco A, Holzknrecht N, Daldrop-Link HE, Rummeny E, Hamm B, Arneson V, Imperatori L, Kirchin MA, Spinazzi A (2000) Evaluation of the accuracy of gadobenate dimeglumine-enhanced MR imaging in the detection and characterization of focal liver lesions. *Am J Roentgenol* 175(4):1111–1120
14. Matsuo M, Kanematsu M, Inaba Y, Matsueda K, Yamagami T, Kondo H, Arai Y, Hoshi H (2001) Pre-operative detection of malignant hepatic tumours: value of combined helical CT during arterial portography and biphasic CT during hepatic arteriography. *Clin Radiol* 56(2):138–145
15. von Herbay A, Vogt C, Haussinger D (2004) Differentiation between benign and malignant hepatic lesions: utility of color stimulated acoustic emission with the microbubble contrast agent Levovist. *J Ultrasound Med* 23(2):207–215
16. Koh DM, Scurr E, Collins DJ, Pirgon A, Kanber B, Karanjia N, Brown G, Leach MO, Husband JE (2006) Colorectal hepatic metastases: quantitative measurements using single-shot echo-planar diffusion-weighted MR imaging. *Eur Radiol* 16(9):1898–1905
17. Taouli B, Vilgrain V, Dumont E, Daire JL, Fan B, Menu Y (2003) Evaluation of liver diffusion isotropy and characterization of focal hepatic lesions with two single-shot echo-planar MR imaging sequences: prospective study in 66 patients. *Radiology* 226(1):71–78
18. Theilmann RJ, Borders R, Trouard TP, Xia G, Outwater E, Ranger-Moore J, Gillies RJ, Stopeck A (2004) Changes in water mobility measured by diffusion MRI predict response of metastatic breast cancer to chemotherapy. *Neoplasia* 6(6):831–837
19. Szafer A, Zhong J, Anderson AW, Gore JC (1995) Diffusion-weighted imaging in tissues: theoretical models. *NMR Biomed* 8:289–296
20. Namimoto T, Yamashita Y, Sumi S, Tang Y, Takahashi M (1997) Focal liver masses: characterization with diffusion-weighted echo-planar MR imaging. *Radiology* 204:739–744
21. Ichikawa T, Haradome H, Hachiya J, Nitatori T, Araki T (1998) Diffusion-weighted MR imaging with a single-shot echoplanar sequence: detection and characterization of focal hepatic lesions. *Am J Roentgenol* 170:397–402